Acta Cryst E CRYSTALLOGRAPHIC COMMUNICATIONS

ISSN 2056-9890

Molecular and crystal structure, Hirshfeld analysis and DFT investigation of 5-(furan-2-ylmethylidene)thiazolo[3,4-*a*]benzimidazole-2-thione

Hafsa Khaldi,[a] Ahmed Djafri,[b,c] Youcef Megrouss,[c] Nawel Khelloul,[c] Abdelkader Chouaih[c]* and Ayada Djafri[a]

[a]Laboratory of Organic Applied Synthesis (LSOA), Department of Chemistry, Faculty of Sciences, University of Oran 1, Ahmed Ben Bella, 31000 Oran, Algeria, [b]Centre de Recherche Scientifique et Technique en Analyses Physico-Chimiques, (CRAPC), BP 384-Bou-Ismail-RP 42004, Tipaza, Algeria, and [c]Laboratory of Technology and Solid Properties (LTPS), Abdelhamid Ibn Badis University, BP 227 Mostaganem 27000, Algeria. *Correspondence e-mail: achouaih@gmail.com

Received 26 October 2020
Accepted 11 November 2020

Edited by M. Weil, Vienna University of Technology, Austria

Keywords: crystal structure; benzimidazoles; thiazoles; DFT analysis; reactivity.

CCDC reference: 2043709

Supporting information: this article has supporting information at journals.iucr.org/e

The thiazolo[3,4-*a*]benzimidazole fused-ring system in the title compound, $C_{14}H_8N_2OS_2$, is nearly planar, the r.m.s. deviation being 0.0073 Å. The thiazolobenzimidazole-2-thione system is almost in the same plane as the furan-2-ylmethylene moiety, with a dihedral angle of 5.6 (2)° between the two least-squares planes. In the crystal, adjacent molecules are connected by weak intermolecular interactions (C—H···N and slipped π–π stacking) into a three-dimensional network. The nature of the intermolecular interactions was also quantified by Hirshfeld surface analysis. DFT analysis indicates a good agreement of the experimentally determined and the theoretically calculated molecular structures.

1. Chemical context

The synthesis and biological activity of thiazolobenzimidazoles were first studied several decades ago (Ogura *et al.*, 1968; Krasovskii & Kochergin, 1972; Alper & Taurins, 1967). With regard to their biological activity, thiazolobenzimidazole derivatives have been evaluated in particular for their inhibitory effects on HIV-1 (Chimirri *et al.*, 1999; Roth *et al.*, 1997) and their use as antibacterial (Oh *et al.*, 1995), anti-inflammatory (Bender *et al.*, 1985), antidiabetic (El-Shorbagi *et al.*, 2001), broncholytic (Park *et al.*, 1993), antiprotozoal (Singh, 1970), anticonvulsant (Sharpe *et al.*, 1971) and antidepressant (Miller & Bambury, 1972) agents. Some thiazolobenzimidazole derivatives are also used for the treatment of cancer and bone diseases (Al-Rashood & Abdel-Aziz, 2010). Furthermore, compounds with the benzimidazole moiety have been developed into useful materials for usage in non-linear optical fields (Vijayan *et al.*, 2004) or photovoltaic cells (Bodedla *et al.*, 2016; Gong *et al.*, 2010).

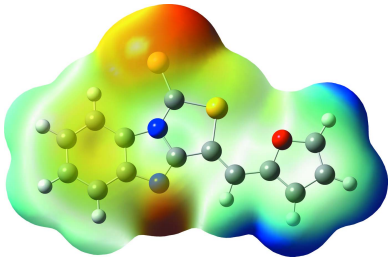

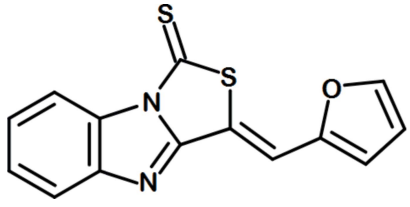

We report in this communication the synthesis, molecular and crystal structures and Hirshfeld surface analysis of the title thiazolo derivative. In addition, the HOMO–LUMO

energies, molecular electrostatic potential and chemical reactivity descriptors are described on the basis of theoretical calculations.

2. Structural commentary

The molecular structure of the title compound is shown in Fig. 1. The tricyclic thiazolobenzimidazole group, consisting of a benzimidazole unit fused to a thiazole ring, is bonded to a furan-2-yl-methylene moiety at carbon atom C6. As expected, the thiazolo[3,4-*a*]benzimidazole group is planar with an r.m.s. deviation of 0.0073 Å for the thirteen (C6–C14/N1/N2/S1/S2) non H-atoms. The furan-2-yl-methylene moiety is also planar, with an r.m.s deviation of 0.0028 Å for the six (C1–C5/O1) non H-atoms. The two ring systems are almost in the same plane, their least-squares planes subtending a dihedral angle of 5.6 (2)°. The molecule exists in a *Z* configuration with respect to the C5═C6 bond. The S1—C8 and S1—C6 distances, 1.739 (4) and 1.775 (3) Å, respectively, are in agreement with a C—S single bond of a thiazole ring (Rahmani *et al.*, 2016). In comparison, the S2—C8 bond [1.612 (4) Å] of the thione moiety is much shorter as a result of its double-bond character and the presence of a delocalized π-electronic system throughout the entire thiazolobenzimidazole ring system (Liang *et al.*, 2009). The bond lengths of the thiazolobenzimidazole and furan rings are similar than those in a series of thiazolo[3,2-*a*]benzimidazole and thiazolo[3,4-*a*]-benzimidazole compounds (Bruno *et al.*, 1996; Wang *et al.*, 2011). The intramolecular C10—H10···S2 hydrogen-bonding interaction (Table 1) helps to stabilize the molecular conformation.

3. Supramolecular features and Hirshfeld surface analysis

In similar reported structures containing thiazole ring systems, the crystal packing is mainly based on short contacts and weak π–π interactions (Djafri *et al.*, 2017). In the crystal packing of the title compound, weak C3—H3$_{aromatic}$···N2^{i} hydrogen bonds (Table 1) connect the molecules into dimers (Fig. 2).

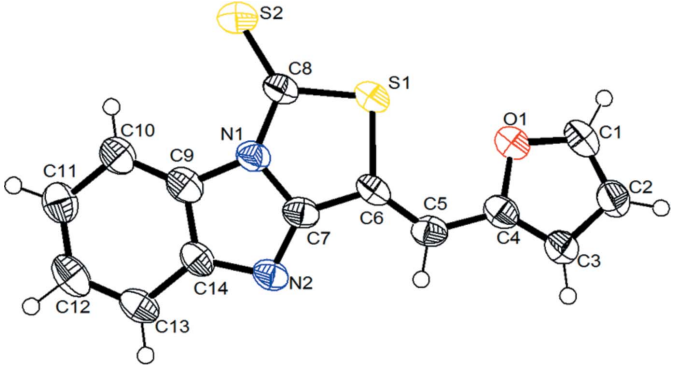

Figure 1
The molecular structure of the title compound showing the atom-numbering scheme. Displacement ellipsoids are drawn at the 50% probability level.

Table 1
Hydrogen-bond geometry (Å, °).

D—H···*A*	*D*—H	H···*A*	*D*···*A*	*D*—H···*A*
C10—H10···S2	0.93	2.94	3.476 (4)	119
C3—H3···N2^{i}	0.93	2.62	3.474 (5)	154
C1—H1···S2^{ii}	0.93	2.89	3.788 (4)	163

Symmetry codes: (i) $-x+\frac{1}{2}, y+\frac{1}{2}, -z+\frac{3}{2}$; (ii) $-x, -y+1, -z+2$.

Additional π–π stacking interactions between adjacent thiazolobenzimidazole ring systems link the dimers into a three-dimensional network structure, with centroid-to-centroid distances of 3.6523 (18) Å (slippage 1.141 Å) and 3.6515 (1) Å (slippage 1.137 Å) between the thiazole ring and the benzene ring of one thiazolobenzimidazole ring system, and between the imidazole ring and the benzene ring of another thiazolobenzimidazole ring system, respectively.

Hirshfeld surface (HS) analysis of the title compound was performed using *Crystal Explorer 17* (Turner *et al.*, 2017) with the surface mapped over d_{norm} as described in the literature (Yahiaoui *et al.*, 2019). In the d_{norm} surface, strong intermolecular interactions appear as red spots (Bahoussi *et al.*, 2017; Khelloul *et al.*, 2016) as depicted in Fig. 3*a* (here originating particularly from the C—H···N hydrogen bond). The presence of π–π stacking interactions is indicated by red and blue triangles on the shape-index surface as can be seen in Fig. 3*b*. In Fig. 3*c*, the other red spots indicate also the presence of a weaker C—H···S hydrogen bond (between H3 and S2) and C—H···N (between H1 and N2). The overall two-dimensional fingerprint (FP) plots, and those delineated into H···H, C···H/H···C, S···H/H···S, N···H/H···N and

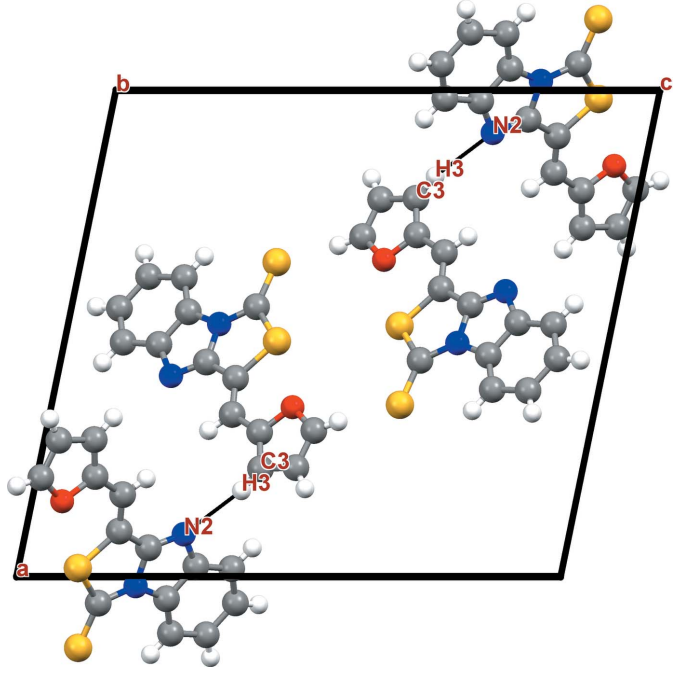

Figure 2
Crystal packing diagram of the title compound with hydrogen bonds (dashed lines) viewed along the *b* axis.

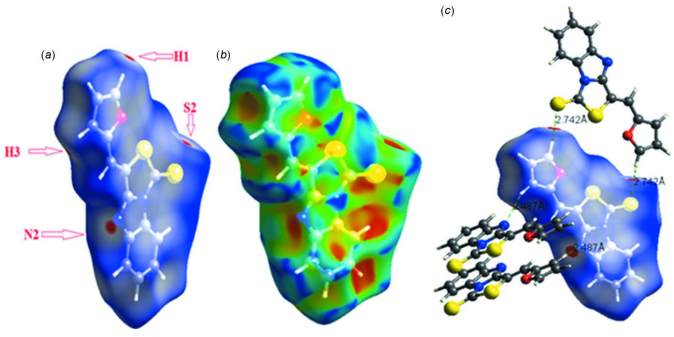

Figure 3
Hirshfeld surfaces for visualizing the intermolecular contacts of the title compound: (*a*) d_{norm} Hirshfeld surface, (*b*) shape-index and (*c*) d_{norm} highlighting the regions of the C—H···S and C—H···N hydrogen bonds.

C···C contacts are shown in Fig. 4. H···H contacts are the dominant interactions with a contribution of 29.8% to the overall HS. The S···H/H···S interactions appear as the next largest region of the FP plot, highly concentrated at the edges, characteristic of hydrogen-bond interactions with an overall HS contribution of 19.6%. The C···H/H···C interactions are illustrated by two symmetrical wings on the left and right sides (16.5% contribution). The C···C contacts, which are the measure of π–π stacking interactions, occupy 9.1% of the HS and appear as a unique triangle. The N···H/H···N contacts are represented by a pair of sharp spikes and make a contribution of 6.6%. Other intermolecular contacts in the HS mapping contribution less than 5%.

4. Theoretical calculations

The hybrid functional B3LYP (Becke's three-parameter hybrid model using the Lee-Yang Parr correlation functional) with the 6-311G (d, p) basis set (Becke, 1993) were used in all calculations as implemented in *Gaussian 09* (Frisch *et al.*, 2009). Theoretical calculations were performed to obtain the optimized molecular structure of the title compound in the gas phase. The crystallographic information file was used as an input file in the *GaussView 5* program (Frisch *et al.*, 2000) to start structure optimization of the title compound. Comparison of the DFT-optimized molecular structure with the refined structure based on single crystal X-ray data revealed a good agreement (see supporting information for a detailed comparison of bond lengths and angles). Frontier molecular orbitals and the molecular electrostatic potential were calculated using the same level of theory.

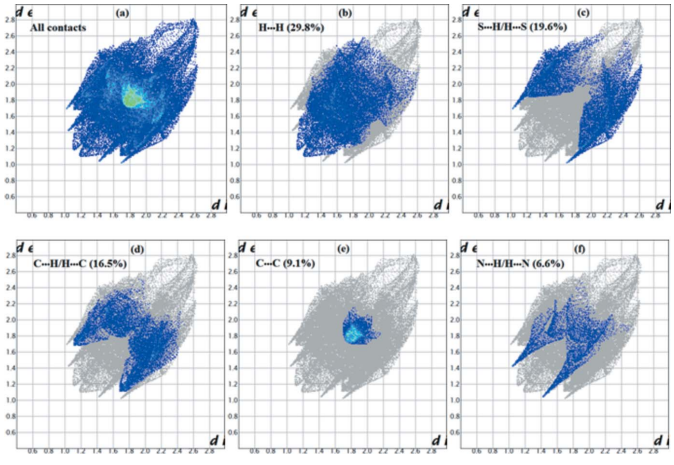

Figure 4
Two-dimensional fingerprint plots showing the contributions of different types of interactions: (*a*) all intermolecular contacts, (*b*) H···H contacts, (*c*) S···H/H···S contacts, (*d*) C···H/H···C contacts, (*e*) C···C contacts and (*f*) N···H/H···N contacts.

5. Frontier molecular orbital and chemical reactivity

The frontier molecular orbitals, HOMO (highest occupied molecular orbital) and LUMO (lowest-unoccupied molecular orbital), are plotted to specify the distribution of electronic densities. The electron distribution of the HOMO-1, HOMO, LUMO and the LUMO+1 energy levels are shown in Fig. 5. As can be seen from the figure, the HOMO and LUMO are localized in the plane extending from the whole furan ring to the thiazolo-benzimidazole ring system. The frontier molecular orbital energies, EHOMO and ELUMO are −7.23 and −1.87 eV, respectively, and the HOMO–LUMO gap is 5.36 eV. Since the gap energy is considered to be small, the molecule is defined as soft.

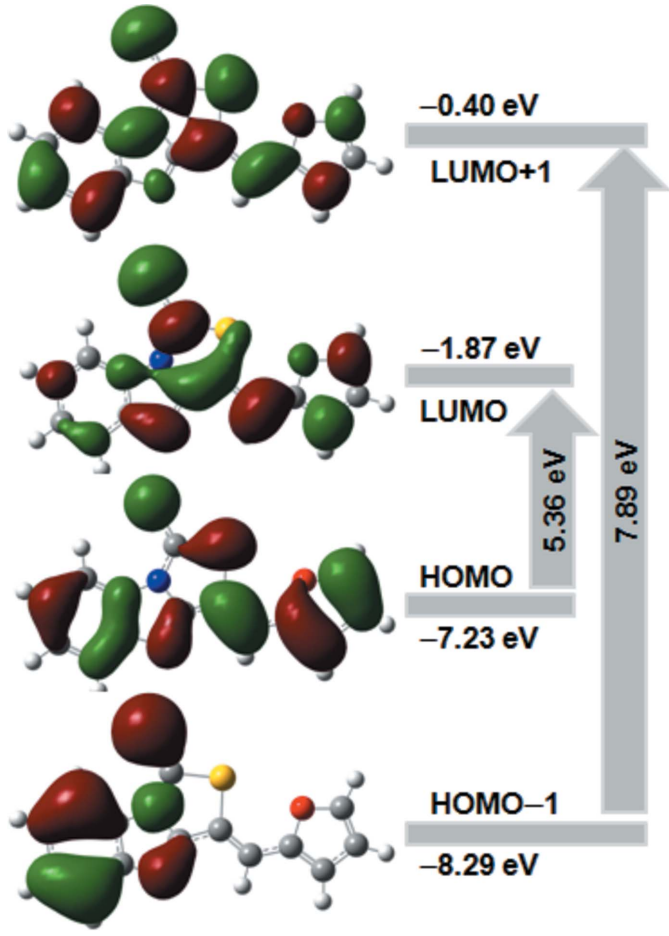

Figure 5
Molecular orbitals plot showing the frontier orbitals.

Table 2
Frontier molecular orbital energies (eV) and global chemical reactivity descriptors calculated using B3LYP/6–311G(d,p) level of theory.

Parameter	Calculated energy
EHOMO	−7.23
ELUMO	−1.87
EHOMO−1	−8.29
ELUMO+1	−0.40
EHOMO–ELUMO (gap)	5.36
EHOMO−1 − ELUMO+1 (gap)	7.89
Ionization potential (I)	7.23
Electron affinity (A)	1.87
Chemical hardness (η)	2.68
Chemical potential (μ)	–4.55
Electronegativity (χ)	4.55
Electrophilicity (ω)	3.86
Hyper-hardness (Γ)	4.30

Global chemical reactivity descriptor (GCRD) parameters can be obtained as reported in the literature (Belkafouf *et al.*, 2019). The calculated values of the GCRD parameters for the title molecule are summarized in Table 2. The chemical stability of the title molecule is explained by the chemical potential (μ) value, which is −4.55 eV. On the other hand, the chemical hardness (η) value is 2.68 eV, indicating that the charge transfer occurs within the molecule. From Table 2, the electrophilic behaviour of the molecule is confirmed by the global electrophilicity (ω), which has a value of 3.86 eV. The structure–property relationship can be also described by the hyper-hardness descriptor (Γ), which was introduced to investigate the reactivity or stability of molecules theoretically (Ghanavatkar *et al.*, 2020). According to the results, the positive value of Γ (+4.30 eV) indicates stability of the molecule.

6. Molecular electrostatic potential analysis

To predict reactive sites for electrophilic and nucleophilic attack, molecular electrostatic potential (MEP) surfaces were computed at the B3LYP/6-311G (d,p) level with the optimized structure using *GaussView* (Frisch *et al.*, 2000). The different values of the electrostatic potential at the MEP surface are represented by red, blue and green (Kourat *et al.*, 2020). From Fig. 6, it is obvious that the negative potential regions (red) are associated with sulfur and nitrogen atoms whereas the positive potential regions (blue) are on the side of hydrogen atoms. It may also be seen in Fig. 6 that green areas cover parts of the molecule enveloping the π system of the aromatic rings.

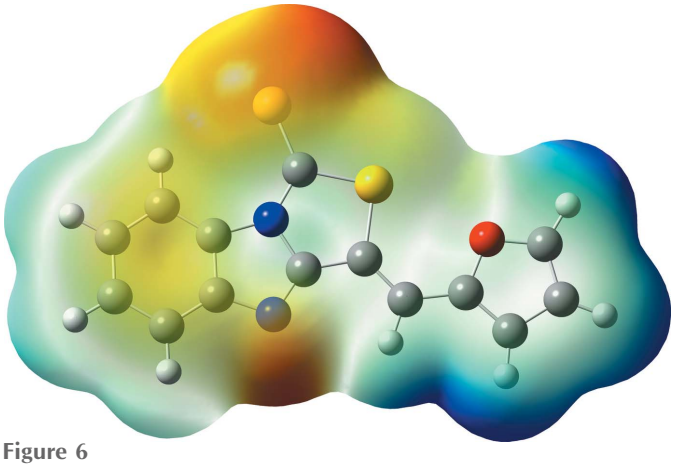

Figure 6
Molecular electrostatic potential map of the title molecule.

7. Synthesis and spectral characterization

The synthetic route preparation of the title compound is illustrated in Fig. 7. Initially, the tricyclic thiazolo(3,4-*a*)benzimidazole (**1**) was obtained from amino phenylene dithiocarbamate and chloroacetic acid by the Hanztsch reaction. The title compound (**3**) was prepared by Knoevenagel condensation of furaldehyde **2** (2; 0.01 mol) and the tricyclic compound (**1**; 0.02 mol) in acetic acid (10 ml) buffered by sodium acetate (0.02 mol). The reaction was monitored by TLC (petroleum ether/ethyl acetate, 8/2). After 4 h of refluxing and stirring, the brown solid obtained was filtered off, dried and recrystallized from ethanol to give the title compound, m.p. 493 K, in a yield of 85%.

Spectroscopic data (FT–IR, ^{1}H NMR and ^{13}C NMR) for (**3**). IR (KBr, cm^{-1}): 3099, 3076 and 3026 (Csp^2—H$_{arom}$), 1602 (C═N), 1555–1464 (C═C), 1390 (C═S), 1324 (–C—S–), 1259 (C—N) and 815, 759 (C—H$_{aryl}$). ^{1}H NMR (300 MHz, $CDCl_3$, δ ppm) J (Hz): 6,6 (*q*, 1H, J_3 = 1.76 Hz, furan), 6.80 (*d*, 1H, J = 3.48 Hz, furan), 7.45 (*m*, 2H, J_3 = 1.66 Hz, J_4 = 5,60 phenyl), 7.60 (*s*, 1H, C═CH), 7.70 (*s*, 1H, furan) , 7.80 (*d*, 1H, J_3 = 8.56 Hz, phenyl), 8.50 (*d*, 1H, J_3 = 8.72 Hz, phenyl). ^{13}C NMR (75 MHz, $CDCl_3$, δ ppm): 113.46, 113.51, 113.90, 117.15, 118.81, 120.65, 121.32, 125.59, 126.55, 131.00, 146.63, 149.48, 150.42 (C═N), 187.15 (C═S).

8. Refinement

Crystal data, data collection and structure refinement details are summarized in Table 3. H atoms were placed in calculated positions (C—H = 0.93 Å) and allowed to ride on their parent atoms with U_{iso}(H) = 1.2U_{eq}(C).

Funding information

The authors gratefully acknowledge financial support *via* the PRFU project from the Algerian Ministry of Higher Education and Scientific Research, the Directorate General of Scientific Research and Technological Development (DGRSDT), Thematic Research Agency in Science and

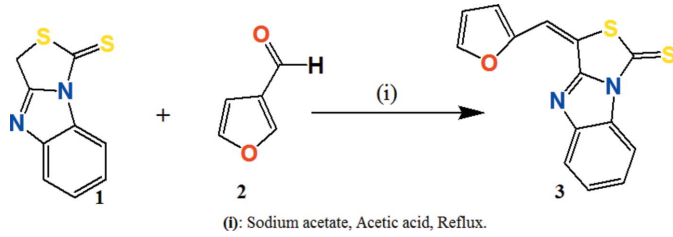

Figure 7
Synthetic route for the title compound (**3**).

Table 3
Experimental details.

Crystal data	
Chemical formula	$C_{14}H_8N_2OS_2$
M_r	284.34
Crystal system, space group	Monoclinic, $P2_1/n$
Temperature (K)	295
a, b, c (Å)	15.768 (5), 4.7583 (15), 17.316 (6)
β (°)	101.572 (8)
V (Å^3)	1272.8 (7)
Z	4
Radiation type	Mo $K\alpha$
μ (mm^{-1})	0.41
Crystal size (mm)	0.58 × 0.21 × 0.20
Data collection	
Diffractometer	Nonius Kappa CCD
Absorption correction	Multi-scan (Blessing, 1995)
T_{min}, T_{max}	0.856, 0.919
No. of measured, independent and observed [$I > 2\sigma(I)$] reflections	10879, 2281, 1835
R_{int}	0.020
(sin $\theta/\lambda)_{max}$ (Å^{-1})	0.602
Refinement	
$R[F^2 > 2\sigma(F^2)]$, $wR(F^2)$, S	0.052, 0.113, 0.96
No. of reflections	2281
No. of parameters	172
H-atom treatment	H-atom parameters constrained
$\Delta\rho_{max}$, $\Delta\rho_{min}$ (e Å^{-3})	0.17, −0.17

Computer programs: *KappaCCD* (Nonius, 1998), *DENZO* and *SCALEPACK* (Otwinowski & Minor, 1997), *SHELXS97* (Sheldrick, 2008), *ORTEP-3 for Windows* (Farrugia, 2012), *Mercury* (Macrae *et al.*, 2020), *SHELXL2014* (Sheldrick, 2015), *PLATON* (Spek, 2020) and *publCIF* (Westrip, 2010).

Technology (ATRST) and Abdelhamid Ibn Badis University of Mostaganem.

References

Alper, A. E. & Taurins, A. (1967). *Can. J. Chem.* **45**, 2903–2912.
Al-Rashood, K. A. & Abdel-Aziz, H. A. (2010). *Molecules*, **15**, 3775–3815.
Bahoussi, R. I., Djafri, A., Chouaih, A., Djafri, A. & Hamzaoui, F. (2017). *Acta Cryst.* E**73**, 173–176.
Becke, A. D. (1993). *J. Chem. Phys.* **98**, 5648–5652.
Belkafouf, N. E. H., Triki Baara, F., Altomare, A., Rizzi, R., Chouaih, A., Djafri, A. & Hamzaoui, F. (2019). *J. Mol. Struct.* **1189**, 8–20.
Bender, P. E., Hill, D., Offen, P. H., Razgaitis, K., Lavanchy, P., Stringer, O. D., Sutton, B. M., Griswold, D. E., DiMartino, M. & Walz, D. T. (1985). *J. Med. Chem.* **28**, 1169–1177.
Blessing, R. H. (1995). *Acta Cryst.* A**51**, 33–38.
Bodedla, G. B., Justin Thomas, K. R., Fan, M. S. & Ho, K. C. (2016). *J. Org. Chem.* **81**, 640–653.
Bruno, G., Chimirri, A., Monforte, A. M., Nicoló, F. & Scopelliti, R. (1996). *Acta Cryst.* C**52**, 2531–2533.
Chimirri, A., Grasso, S., Monforte, P., Rao, A., Zappalà, M., Monforte, A. M., Pannecouque, C., Witvrouw, M., Balzarini, J. & De Clercq, E. (1999). *Antivir. Chem. Chemother.* **10**, 211–217.
Djafri, A., Chouaih, A., Daran, J.-C., Djafri, A. & Hamzaoui, F. (2017). *Acta Cryst.* E**73**, 511–514.
El-Shorbagi, A., Hayallah, A. A., Omar, N. M. & Ahmed, A. N. (2001). *Bull. Pharm. Sci. Assiut*, **24**, 7–20.
Farrugia, L. J. (2012). *J. Appl. Cryst.* **45**, 849–854.
Frisch, A., Nielson, A. B. & Holder, A. J. (2000). *GAUSSVIEW User Manual*. Gaussian Inc, Pittsburgh.
Frisch, M. J., Trucks, G. W., Schlegel, H. B., Scuseria, G. E., Robb, M. A., Cheeseman, J. R., Scalmani, G., Barone, V., Mennucci, B., Petersson, G. A., Nakatsuji, H., Caricato, M., Li, X., Hratchian, H. P., Izmaylov, A. F., Bloino, J., Zheng, G., Sonnenberg, J. L., Hada, M., Ehara, M., Toyota, K., Fukuda, R., Hasegawa, J., Ishida, M., Nakajima, T., Honda, Y., Kitao, O., Nakai, H., Vreven, T., Montgomery, J. A. Jr, Peralta, J. E., Ogliaro, F., Bearpark, M., Heyd, J. J., Brothers, E., Kudin, K. N., Staroverov, V. N., Kobayashi, R., Normand, J., Raghavachari, K., Rendell, A., Burant, J. C., Iyengar, S. S., Tomasi, J., Cossi, M., Rega, N., Millam, J. M., Klene, M., Knox, J. E., Cross, J. B., Bakken, V., Adamo, C., Jaramillo, J., Gomperts, R., Stratmann, R. E., Yazyev, O., Austin, A. J., Cammi, R., Pomelli, C., Ochterski, J. W., Martin, R. L., Morokuma, K., Zakrzewski, V. G., Voth, G. A., Salvador, P., Dannenberg, J. J., Dapprich, S., Daniels, A. D., Farkas, Ö., Foresman, J. B., Ortiz, J. V., Cioslowski, J. & Fox, D. J. (2009). *GAUSSIAN09*. Gaussian Inc., Wallingford, CT, USA.
Ghanavatkar, C. W., Mishra, V. R., Sekar, N., Mathew, E., Thomas, S. S. & Joe, I. H. (2020). *J. Mol. Struct.* **1203**, 127401.
Gong, S., Zhao, Y., Yang, C., Zhong, C., Qin, J. & Ma, D. (2010). *J. Phys. Chem.* C**114**, 5193–5198.
Khelloul, N., Toubal, K., Benhalima, N., Rahmani, R., Chouaih, A., Djafri, A. & Hamzaoui, F. (2016). *Acta Chim. Slov.* **63**, 619–626.
Kourat, O., Djafri, A., Benhalima, N., Megrouss, Y., Belkafouf, N. E. H., Rahmani, R., Daran, J.-C., Djafri, A. & Chouaih, A. (2020). *J. Mol. Struct.* **1222**, 128952.
Krasovskii, A. N. & Kochergin, P. M. (1972). *Chem. Heterocycl. Compd.* **5**, 243–245.
Liang, Y., He, H.-W. & Yang, Z.-W. (2009). *Acta Cryst.* E**65**, o3098.
Macrae, C. F., Sovago, I., Cottrell, S. J., Galek, P. T. A., McCabe, P., Pidcock, E., Platings, M., Shields, G. P., Stevens, J. S., Towler, M. & Wood, P. A. (2020). *J. Appl. Cryst.* **53**, 226–235.
Miller, L. F. & Bambury, R. E. (1972). *J. Med. Chem.* **15**, 415–417.
Nonius (1998). *KappaCCD Reference Manual*. Nonius BV, Delft, The Netherlands.
Ogura, H., Itoh, T. & Tajika, T. (1968). *J. Heterocycl. Chem.* **5**, 319–322.
Oh, C., Ham, Y., Hong, S. & Cho, J. (1995). *Arch. Pharm. Pharm. Med. Chem.* **328**, 289–291.
Otwinowski, Z. & Minor, W. (1997). *Methods in Enzymology*, Vol. 276, *Macromolecular Crystallography*, Part A, edited by C. W. Carter Jr & R. M. Sweet, pp. 307–326. New York: Academic Press.
Park, Y. J., Such, K. H., Kang, E. C., Yoon, H. S., Kim, Y. H., Kang, D. P. & Chang, M. S. (1993). *Korean J. Med. Chem.* **3**, 124–129.
Rahmani, R., Djafri, A., Daran, J.-C., Djafri, A., Chouaih, A. & Hamzaoui, F. (2016). *Acta Cryst.* E**72**, 155–157.
Roth, T., Morningstar, M. L., Boyer, P. L., Hughes, S. H., Buckheit, R. W. Jr & Michejda, C. J. (1997). *J. Med. Chem.* **40**, 4199–4207.
Sharpe, C. J., Shadbolt, R. S., Ashford, A. & Ross, J. W. (1971). *J. Med. Chem.* **14**, 977–982.
Sheldrick, G. M. (2008). *Acta Cryst.* A**64**, 112–122.
Sheldrick, G. M. (2015). *Acta Cryst.* C**71**, 3–8.
Singh, J. M. (1970). *J. Med. Chem.* **13**, 1018.
Spek, A. L. (2020). *Acta Cryst.* E**76**, 1–11.
Turner, M. J., Mckinnon, J. J., Wolff, S. K., Grimwood, D. J., Spackman, P. R., Jayatilaka, D. & Spackman, M. A. (2017). *Crystal Explorer 17*. The University of Western Australia.
Vijayan, N., Ramesh Babu, R., Gopalakrishnan, R., Ramasamy, P. & Harrison, W. T. A. (2004). *J. Cryst. Growth*, **262**, 490–498.
Wang, Z.-M., Yu, B., Cui, Y., Zhang, X.-Q. & Sun, X.-Q. (2011). *Acta Cryst.* E**67**, o2540.
Westrip, S. P. (2010). *J. Appl. Cryst.* **43**, 920–925.
Yahiaoui, S., Moliterni, A., Corriero, N., Cuocci, C., Toubal, K., Chouaih, A., Djafri, A. & Hamzaoui, F. (2019). *J. Mol. Struct.* **1177**, 186–192.

supporting information

Acta Cryst. (2020). E**76**, 1832-1836 [https://doi.org/10.1107/S2056989020015017]

Molecular and crystal structure, Hirshfeld analysis and DFT investigation of 5-(furan-2-ylmethylidene)thiazolo[3,4-*a*]benzimidazole-2-thione

Hafsa Khaldi, Ahmed Djafri, Youcef Megrouss, Nawel Khelloul, Abdelkader Chouaih and Ayada Djafri

Computing details

Data collection: *KappaCCD* (Nonius, 1998); cell refinement: *DENZO* and *SCALEPACK* (Otwinowski & Minor, 1997); data reduction: *DENZO* and *SCALEPACK* (Otwinowski & Minor, 1997); program(s) used to solve structure: *SHELXS97* (Sheldrick, 2008); program(s) used to refine structure: *SHELXL2014* (Sheldrick, 2015); molecular graphics: *ORTEP-3 for Windows* (Farrugia, 2012), *Mercury* (Macrae *et al.*, 2020); software used to prepare material for publication: *SHELXL2014* (Sheldrick, 2015), *PLATON* (Spek, 2020) and *publCIF* (Westrip, 2010).

5-(Furan-2-ylmethylidene)thiazolo[3,4-*a*]benzimidazole-2-thione

Crystal data

$C_{14}H_8N_2OS_2$
$M_r = 284.34$
Monoclinic, $P2_1/n$
$a = 15.768$ (5) Å
$b = 4.7583$ (15) Å
$c = 17.316$ (6) Å
$\beta = 101.572$ (8)°
$V = 1272.8$ (7) Å^3
$Z = 4$
$F(000) = 584$
$D_x = 1.484$ Mg m^{-3}
Mo $K\alpha$ radiation, $\lambda = 0.71073$ Å
Cell parameters from 100 reflections
$\theta = 2.0$–$25.3°$
$\mu = 0.41$ mm^{-1}
$T = 295$ K
Prism, colourless
0.58 × 0.21 × 0.20 mm

Data collection

Nonius Kappa CCD diffractometer
Radiation source: sealed tube
$\theta/2\theta$ scans
Absorption correction: multi-scan (Blessing, 1995)
$T_{min} = 0.856$, $T_{max} = 0.919$
10879 measured reflections
2281 independent reflections
1835 reflections with $I > 2\sigma(I)$
$R_{int} = 0.020$
$\theta_{max} = 25.4°$, $\theta_{min} = 3.6°$
$h = -18\rightarrow18$
$k = -5\rightarrow5$
$l = -20\rightarrow20$

Refinement

Refinement on F^2
Least-squares matrix: full
$R[F^2 > 2\sigma(F^2)] = 0.052$
$wR(F^2) = 0.113$
$S = 0.96$
2281 reflections
172 parameters
0 restraints
Hydrogen site location: inferred from neighbouring sites
H-atom parameters constrained

$w = 1/[\sigma^2(F_o^2) + (0.0089P)^2 + 4.0499P]$
where $P = (F_o^2 + 2F_c^2)/3$
$(\Delta/\sigma)_{max} < 0.001$

$\Delta\rho_{max} = 0.17$ e Å^{-3}
$\Delta\rho_{min} = -0.17$ e Å^{-3}

Special details

Geometry. All esds (except the esd in the dihedral angle between two l.s. planes) are estimated using the full covariance matrix. The cell esds are taken into account individually in the estimation of esds in distances, angles and torsion angles; correlations between esds in cell parameters are only used when they are defined by crystal symmetry. An approximate (isotropic) treatment of cell esds is used for estimating esds involving l.s. planes.

Fractional atomic coordinates and isotropic or equivalent isotropic displacement parameters (Å²)

	x	*y*	*z*	U_{iso}*/U_{eq}
S1	0.01611 (6)	0.1179 (2)	0.89016 (5)	0.0504 (3)
S2	−0.14717 (8)	−0.2152 (3)	0.85975 (7)	0.0732 (4)
O1	0.15244 (16)	0.5043 (6)	0.94349 (14)	0.0523 (7)
C14	0.0218 (2)	−0.4142 (8)	0.67488 (18)	0.0432 (9)
N1	−0.01982 (18)	−0.2326 (7)	0.77765 (15)	0.0436 (7)
C9	−0.0453 (2)	−0.4245 (9)	0.71658 (19)	0.0467 (9)
C7	0.0587 (2)	−0.1218 (8)	0.76838 (19)	0.0427 (9)
C11	−0.1192 (3)	−0.7634 (9)	0.6302 (2)	0.0536 (10)
H11	−0.1661	−0.8825	0.6139	0.064*
N2	0.08686 (18)	−0.2264 (7)	0.70874 (15)	0.0430 (7)
C8	−0.0552 (2)	−0.1294 (9)	0.83946 (19)	0.0467 (9)
C13	0.0170 (2)	−0.5792 (9)	0.60819 (19)	0.0485 (10)
H13	0.0595	−0.5718	0.5780	0.058*
C6	0.0923 (2)	0.0822 (8)	0.82795 (19)	0.0430 (9)
C5	0.1667 (2)	0.2165 (8)	0.8349 (2)	0.0433 (9)
H5	0.1996	0.1713	0.7976	0.052*
C3	0.2789 (2)	0.5589 (8)	0.9074 (2)	0.0490 (9)
H3	0.3240	0.5411	0.8804	0.059*
C10	−0.1160 (2)	−0.5960 (9)	0.6964 (2)	0.0503 (10)
H10	−0.1595	−0.6002	0.7255	0.060*
C4	0.2034 (2)	0.4222 (8)	0.8920 (2)	0.0462 (9)
C1	0.2005 (3)	0.6951 (9)	0.9914 (2)	0.0551 (10)
H1	0.1822	0.7867	1.0326	0.066*
C2	0.2770 (3)	0.7349 (9)	0.9723 (2)	0.0540 (10)
H2	0.3206	0.8552	0.9969	0.065*
C12	−0.0534 (3)	−0.7544 (9)	0.5885 (2)	0.0574 (11)
H12	−0.0568	−0.8722	0.5452	0.069*

Atomic displacement parameters (Å²)

	U^{11}	U^{22}	U^{33}	U^{12}	U^{13}	U^{23}
S1	0.0569 (6)	0.0590 (6)	0.0373 (5)	−0.0007 (5)	0.0142 (4)	−0.0071 (5)
S2	0.0644 (7)	0.0958 (10)	0.0690 (7)	−0.0167 (7)	0.0360 (6)	−0.0209 (7)
O1	0.0584 (16)	0.0575 (17)	0.0423 (14)	−0.0015 (14)	0.0132 (12)	−0.0078 (13)
C14	0.053 (2)	0.047 (2)	0.0274 (16)	0.0062 (19)	0.0031 (15)	0.0015 (17)
N1	0.0464 (17)	0.0520 (19)	0.0331 (15)	0.0008 (15)	0.0099 (13)	0.0005 (14)

C9	0.052 (2)	0.052 (2)	0.0342 (18)	0.0062 (19)	0.0032 (16)	0.0032 (18)
C7	0.048 (2)	0.050 (2)	0.0316 (17)	0.0049 (18)	0.0099 (15)	0.0058 (17)
C11	0.058 (2)	0.058 (3)	0.040 (2)	0.000 (2)	−0.0011 (17)	−0.003 (2)
N2	0.0497 (17)	0.0521 (19)	0.0271 (14)	0.0028 (15)	0.0079 (13)	0.0038 (14)
C8	0.052 (2)	0.056 (2)	0.0347 (18)	0.0025 (19)	0.0132 (16)	−0.0015 (18)
C13	0.060 (2)	0.056 (3)	0.0300 (17)	0.009 (2)	0.0082 (16)	0.0036 (18)
C6	0.049 (2)	0.049 (2)	0.0316 (17)	0.0033 (19)	0.0103 (15)	−0.0033 (17)
C5	0.054 (2)	0.040 (2)	0.0389 (18)	0.0017 (18)	0.0157 (16)	0.0063 (17)
C3	0.055 (2)	0.053 (3)	0.0399 (19)	−0.003 (2)	0.0102 (17)	−0.0020 (18)
C10	0.057 (2)	0.058 (3)	0.0334 (18)	0.004 (2)	0.0020 (16)	0.0011 (19)
C4	0.055 (2)	0.046 (2)	0.0377 (19)	0.0021 (19)	0.0106 (16)	0.0023 (18)
C1	0.069 (3)	0.055 (3)	0.041 (2)	0.003 (2)	0.0097 (19)	−0.010 (2)
C2	0.061 (2)	0.057 (3)	0.041 (2)	−0.006 (2)	0.0041 (18)	−0.006 (2)
C12	0.072 (3)	0.059 (3)	0.037 (2)	0.013 (2)	−0.0003 (19)	−0.008 (2)

Geometric parameters (Å, º)

S1—C8	1.739 (4)	C11—C10	1.388 (5)
S1—C6	1.775 (3)	C11—H11	0.9300
S2—C8	1.612 (4)	C13—C12	1.376 (6)
O1—C1	1.354 (5)	C13—H13	0.9300
O1—C4	1.372 (4)	C6—C5	1.320 (5)
C14—C13	1.386 (5)	C5—C4	1.429 (5)
C14—C9	1.397 (5)	C5—H5	0.9300
C14—N2	1.397 (5)	C3—C4	1.336 (5)
N1—C7	1.384 (4)	C3—C2	1.407 (5)
N1—C8	1.392 (4)	C3—H3	0.9300
N1—C9	1.394 (5)	C10—H10	0.9300
C9—C10	1.368 (5)	C1—C2	1.326 (5)
C7—N2	1.302 (4)	C1—H1	0.9300
C7—C6	1.438 (5)	C2—H2	0.9300
C11—C12	1.378 (5)	C12—H12	0.9300
C8—S1—C6	94.40 (17)	C5—C6—C7	125.8 (3)
C1—O1—C4	105.1 (3)	C5—C6—S1	126.6 (3)
C13—C14—C9	119.3 (4)	C7—C6—S1	107.6 (3)
C13—C14—N2	128.7 (3)	C6—C5—C4	128.6 (3)
C9—C14—N2	112.0 (3)	C6—C5—H5	115.7
C7—N1—C8	117.4 (3)	C4—C5—H5	115.7
C7—N1—C9	106.9 (3)	C4—C3—C2	106.7 (3)
C8—N1—C9	135.7 (3)	C4—C3—H3	126.6
C10—C9—N1	132.9 (3)	C2—C3—H3	126.6
C10—C9—C14	123.5 (3)	C9—C10—C11	116.5 (4)
N1—C9—C14	103.6 (3)	C9—C10—H10	121.8
N2—C7—N1	113.7 (3)	C11—C10—H10	121.8
N2—C7—C6	133.7 (3)	C3—C4—O1	110.3 (3)
N1—C7—C6	112.6 (3)	C3—C4—C5	133.8 (3)
C12—C11—C10	120.5 (4)	O1—C4—C5	115.9 (3)

C12—C11—H11	119.7	C2—C1—O1	111.6 (3)
C10—C11—H11	119.7	C2—C1—H1	124.2
C7—N2—C14	103.8 (3)	O1—C1—H1	124.2
N1—C8—S2	126.5 (3)	C1—C2—C3	106.3 (4)
N1—C8—S1	108.0 (3)	C1—C2—H2	126.8
S2—C8—S1	125.5 (2)	C3—C2—H2	126.8
C12—C13—C14	117.1 (4)	C13—C12—C11	123.0 (4)
C12—C13—H13	121.4	C13—C12—H12	118.5
C14—C13—H13	121.4	C11—C12—H12	118.5

C7—N1—C9—C10	179.5 (4)	N2—C14—C13—C12	178.0 (4)
C8—N1—C9—C10	−3.1 (7)	N2—C7—C6—C5	−0.5 (7)
C7—N1—C9—C14	0.3 (4)	N1—C7—C6—C5	178.3 (4)
C8—N1—C9—C14	177.7 (4)	N2—C7—C6—S1	179.8 (4)
C13—C14—C9—C10	1.7 (6)	N1—C7—C6—S1	−1.4 (4)
N2—C14—C9—C10	−178.7 (3)	C8—S1—C6—C5	−179.0 (4)
C13—C14—C9—N1	−179.0 (3)	C8—S1—C6—C7	0.7 (3)
N2—C14—C9—N1	0.6 (4)	C7—C6—C5—C4	179.5 (4)
C8—N1—C7—N2	−179.2 (3)	S1—C6—C5—C4	−0.9 (6)
C9—N1—C7—N2	−1.2 (4)	N1—C9—C10—C11	−179.7 (4)
C8—N1—C7—C6	1.8 (5)	C14—C9—C10—C11	−0.7 (6)
C9—N1—C7—C6	179.7 (3)	C12—C11—C10—C9	0.5 (6)
N1—C7—N2—C14	1.5 (4)	C2—C3—C4—O1	0.7 (4)
C6—C7—N2—C14	−179.7 (4)	C2—C3—C4—C5	−179.5 (4)
C13—C14—N2—C7	178.2 (4)	C1—O1—C4—C3	−0.6 (4)
C9—C14—N2—C7	−1.3 (4)	C1—O1—C4—C5	179.5 (3)
C7—N1—C8—S2	177.2 (3)	C6—C5—C4—C3	175.6 (4)
C9—N1—C8—S2	0.0 (6)	C6—C5—C4—O1	−4.5 (6)
C7—N1—C8—S1	−1.2 (4)	C4—O1—C1—C2	0.2 (4)
C9—N1—C8—S1	−178.4 (3)	O1—C1—C2—C3	0.2 (5)
C6—S1—C8—N1	0.3 (3)	C4—C3—C2—C1	−0.5 (5)
C6—S1—C8—S2	−178.1 (3)	C14—C13—C12—C11	2.4 (6)
C9—C14—C13—C12	−2.5 (5)	C10—C11—C12—C13	−1.4 (6)

Hydrogen-bond geometry (Å, º)

D—H···*A*	*D*—H	H···*A*	*D*···*A*	*D*—H···*A*
C10—H10···S2	0.93	2.94	3.476 (4)	119
C3—H3···N2^{i}	0.93	2.62	3.474 (5)	154
C1—H1···S2^{ii}	0.93	2.89	3.788 (4)	163

Symmetry codes: (i) −*x*+1/2, *y*+1/2, −*z*+3/2; (ii) −*x*, −*y*+1, −*z*+2.